Available online at www.sciencedirect.com
ScienceDirect
Journal of Nuclear Materials 373 (2008) 179–185
journal of nuclear materials
www.elsevier.com/locate/jnucmat

Anisotropic delayed hydride cracking velocity of CANDU Zr–2.5Nb pressure tubes

Young Suk Kim *, Yong Moo Cheong

Zirconium Team, Korea Atomic Energy Research Institute, 150, Dukjin-dong, Yuseong, Daejeon 305-353, Republic of Korea

Received 16 December 2006; accepted 25 May 2007

Abstract

Delayed hydride cracking (DHC) tests were conducted on CANDU[1] Zr–2.5Nb tubes containing hydrogen with a microstructure of elongated α-Zr and semi-continuous β-Zr at temperatures ranging from 100 to 300 °C. DHC velocity (DHCV) was found to be around two times higher in the axial direction than that in the radial direction even on the same cracking plane. According to Kim's DHC model that DHCV at temperatures lower than 300 °C is governed mainly by hydrogen diffusion and to a lesser extent by the hydrogen concentration gradient at the crack tip, we suggest that the enhanced DHCV in the axial direction arises from a faster hydrogen diffusion in the axial direction with a semi-continuous distribution of β-Zr. Evidence to this suggestion is provided by Levi's experiment that Zr–2.5Nb tubes or plates with a fully discontinuous β-Zr due to annealing at 400 °C for 1000 h or 650 °C for 9 h has no anisotropic DHCV with the orientation. Hence, we conclude that Kim's DHC model is plausible. An anisotropic DHCV of irradiated CANDU Zr–2.5Nb tubes is discussed based on their microstructural evolution with the neutron fluence and operating temperatures.

PACS: 81.40.Np

1. Introduction

Since many failures of Zr–2.5Nb pressure tubes by delayed hydride cracking (DHC) were reported in Pickering 3 and 4 nuclear power plants in 1974 [1], one of the items to be examined during regular overhauls of operating CANadian Deuterium Uranium (CANDU) reactors is if the surface flaws will grow by delayed hydride cracking (DHC) to through-wall cracks. Further, the size of the flaws should be evaluated by accounting for anisotropic DHC velocity (DHCV) till the evaluation period in order to assure the mechanical integrity of the pressure tubes. It should be noted that DHCV is faster in the axial direction of the CANDU Zr–2.5Nb pressure tubes than that in the radial direction. According to Sagat's result [2], especially, irradiated CANDU pressure tubes showed a strong temperature dependency of the anisotropic DHCV which surprisingly disappeared at as high a temperature as 300 °C.

According to previous DHC models that a driving force for DHC is a stress gradient [3,4], an anisotropic DHCV and its temperature dependency in CANDU pressure tubes cannot be satisfactorily understood. By demonstrating a larger extent of the textural change and higher strain hardening after yielding in the axial direction of a CANDU Zr–2.5Nb pressure tube when compared to that in the radial direction, Kim suggested that a steeper stress gradient ahead of the crack tip in the axial direction is the cause of an anisotropic DHCV with orientation [5]. However, his hypothesis has some defects because it was suggested based on the previous DHC models. Recently, Kim has proposed a new DHC model that the driving force for DHC is not a stress gradient but a hydrogen concentration gradient induced by a stress-induced precipitation of hydrides at the crack tip and DHCV is governed by the product of a hydrogen diffusion and a hydrogen concentration gradient

* Corresponding author. Tel.: +82 42 868 2359; fax: +82 42 868 8346.
E-mail address: yskim1@kaeri.re.kr (Y.S. Kim).
[1] CANadian Deuterium Uranium.

0022-3115/$ - see front matter © 2007 Elsevier B.V. All rights reserved.
doi:10.1016/j.jnucmat.2007.05.047

[6–8]. Furthermore, by comparing DHCV of Zr–2.5Nb tubes with different distributions of the β-Zr phase and yield strengths, Kim demonstrated that hydrogen diffusion mainly governs DHCV at below 300 °C [9]. Thus, Kim's new DHC model implicitly suggests that the anisotropic DHCV in CANDU pressure tubes may be attributed to an anisotropic hydrogen diffusion in the corresponding temperature range.

The aim of this study is to elucidate the cause of an anisotropic DHCV in CANDU pressure tubes by correlating it with hydrogen diffusion with orientation and thereby to demonstrate the plausibility of Kim's DHC model [6–8]. To this end, we determined axial and radial DHCV's using compact tension and cantilever beam specimens containing hydrogen which were taken from a CANDU pressure tube with an anisotropic distribution of the β-Zr. As decisive evidence for the role of an anisotropic hydrogen diffusion in the anisotropic DHCV, we cited Levi and Sagat's experiment [10] where DHC tests were conducted on annealed Zr–2.5Nb tubes and plates with a fully discontinuous β-Zr.

2. Experimental procedures

2.1. Materials

Compact tension (CT) specimens of 17 mm long and cantilever beam (CB) specimens of 38 mm long, as shown in Fig. 1, were taken from a CANDU Zr–2.5Nb tube with elongated α-Zr grains in the axial direction. According to the microstructural analyses by TEM and SEM, the CANDU Zr–2.5Nb tube had the non-uniform distribution of the β-Zr phase lying semi-continuously between the elongated α-Zr grains in the axial direction of the tube (Fig. 2(a), which appears white on the SEM, as shown in Fig. 2(b). The compact tension and cantilever beam specimens were used for determining the DHC velocities and the threshold stress intensity factors, K_{IH}'s for the onset of delayed hydride cracking, respectively, in the axial and radial directions of the CANDU Zr–2.5Nb tube. Both the specimens were not given any prior heat treatments to affect the distribution of the β-Zr phase. All the specimens were subjected to electrolytic charging to form a thick hydride layer on their surface followed by homogenization treatment at different temperatures to dissolve hydrogen concentration ranging from 27 to 100 ppm H. At the end of homogenization treatment, they were water-quenched or furnace-cooled to change the size and phase of the hydride precipitates. The details of the hydrogen charging procedures have been reported elsewhere [11]. The real hydrogen content of the specimen was obtained by averaging a set of 5–7 data measured with a LECO RH 404 analyzer. A pre-fatigue crack of 1.7 mm was introduced using an Instron 8501 for the CT specimens to set the ratio of the pre-fatigue crack length and the specimen length or a_o/W equal to 0.5, but not for the CB specimens. The CB specimens had just a sharp notch of 0.5 mm depth in the radial direction with the crack tip radius of 0.05 mm since the DHC velocity was found to be unaffected by a notch tip size smaller than 0.15 mm [12].

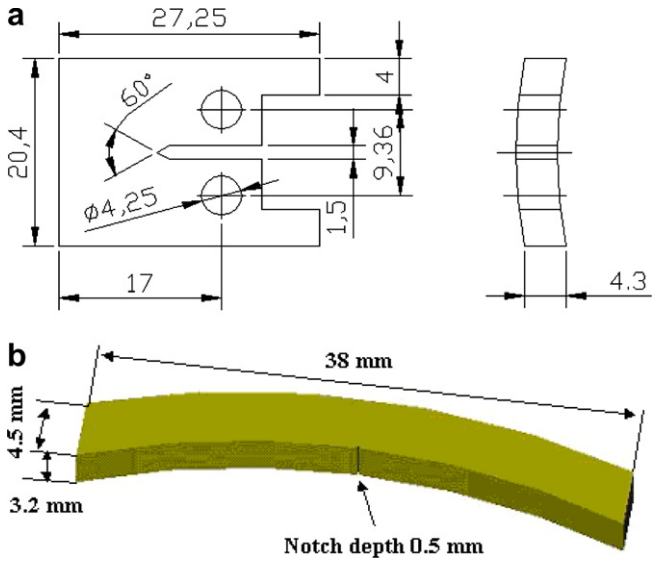

Fig. 1. Schematic drawings of (a) 17 mm compact tension specimens and (b) 38 mm cantilever beam specimens used for the delayed hydride cracking tests in the axial and radial directions of a CANDU Zr–2.5Nb tube.

2.2. DHC tests

DHC tests were conducted using a creep machine to apply a constant load to the 17 mm CT specimens or using a cantilever beam tester to apply constant stress intensity factors to the CB specimens with a 0.5 mm deep notch and the notch root radius of 0.05 mm, as shown in Fig. 1. The initiation and growth of a crack was monitored by a direct current potential drop method for the CT specimens and by an acoustic emission method for the CB specimens. The stress intensity factor ranging from 6.13 to 18.4 MPa$\sqrt{m}$ was applied during the DHC tests on the CB specimens through an auto-control program where the applied load was reduced in proportion to the crack length obtained from the cumulative AE counts using a step-motor [13,14]. Most of the specimens were subjected to a thermal cycle during the DHC tests where the test temperatures were approached from an upward direction by a cooling as shown in Fig. 3. The specimens were heated up to a peak temperature by 0.5–1 °C/min., held there for 1–20 h and cooled down to the test temperature followed by applying a load 30 min after reaching the test temperature. The peak temperature was set at 10 °C higher than the TSSD temperature to completely dissolve all the charged hydrogen. The water-quenched specimens after a homogenization treatment of hydrogen were not subjected to a thermal cycle but they approached the test temperature directly by a heating. The threshold stress intensity factor, K_{IH} was determined by the load-decreasing mode [2] where the applied load decreased from 20 MPa$\sqrt{m}$ step-wise by

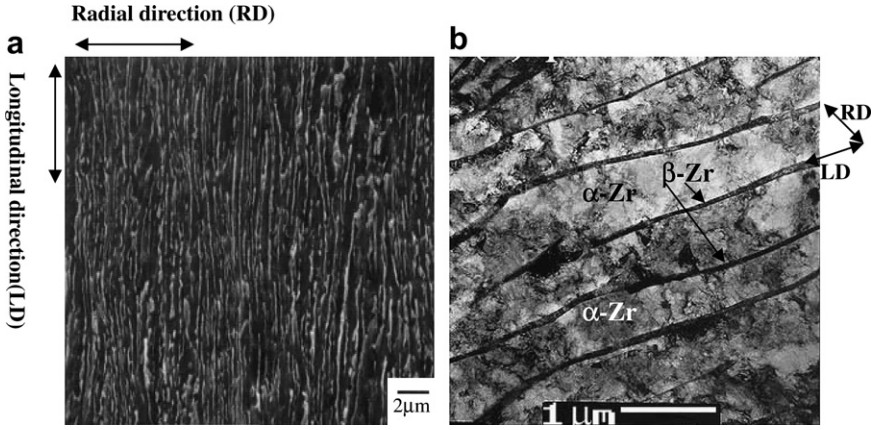

Fig. 2. Microstructures of a CANDU Zr–2.5Nb tube when examined by (a) SEM and (b) TEM, respectively. The β-Zr appeared as white and continuous lines running along the axial direction of the tube (a) and lay in between the elongated α-Zr grains (b).

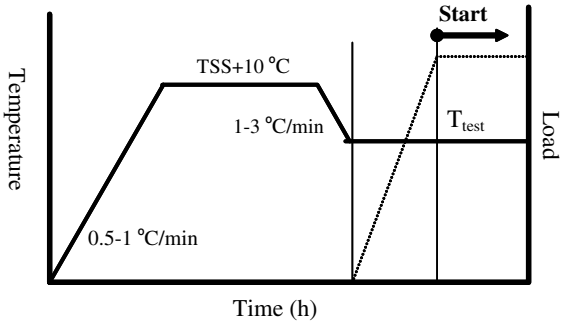

Fig. 3. Diagram of a thermal cycle and loading schedule applied during the DHC tests.

0.5 MPa$\sqrt{m}$ until the crack growth stopped. More than 2 measured data were obtained at each test temperature for the reliability of the K_{IH} data. DHCV was determined from post-fracture measurements of the DHC crack length by an image analyzer method divided by the cracking time.

3. Results and discussion

3.1. Anisotropic DHCV of an unirradiated CANDU Zr–2.5Nb tube

Fig. 4 shows the measured DHCV in the axial and radial directions of the CANDU Zr–2.5Nb tube at temperatures ranging from 100 to 300 °C. As expected, the axial DHCV was around 1.8–2 times higher than the radial DHCV and the difference between the radial DHCV and the axial one remained constant over a temperature range of 160–250 °C. This constant difference in DHCV with the orientation agrees with Sagat's anisotropic DHCV data for an unirradiated CANDU Zr–2.5Nb tube but it differs from that for irradiated CANDU Zr–2.5Nb tubes [2]. Fig. 5 shows the threshold stress intensity factors, K_{IH}'s for the onset of delayed hydride cracking that were determined for the axial and radial directions of the CANDU Zr–

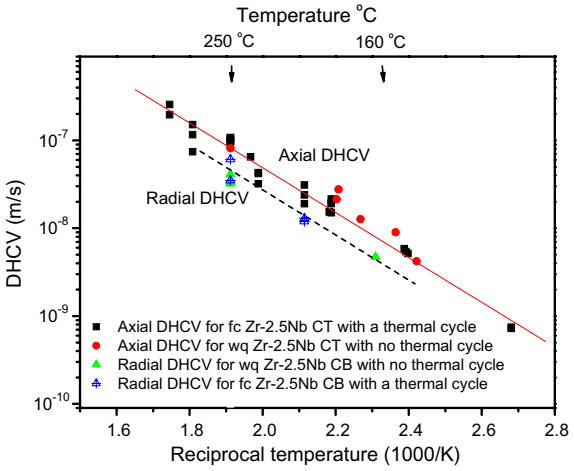

Fig. 4. DHC velocity of a CANDU Zr–2.5Nb tube with the orientation: fc and wq represent acronyms of furnace-cooled and water-quenched while a thermal cycle and no thermal cycle are the heat treatments with the test temperature approached by a cooling and by a heating without a cooling, respectively.

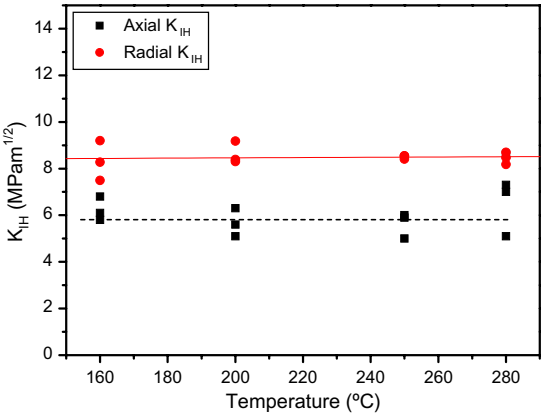

Fig. 5. Threshold stress intensity factor, K_{IH} for the onset of DHC for a CANDU Zr–2.5Nb tube with the orientation that were determined by the load-decreasing mode.

2.5Nb tube at temperatures ranging from 160 to 280 °C. The radial K_{IH} was higher than the axial K_{IH} and the ratio of the radial and axial K_{IH} was kept constant in this temperature interval.

According to Kim's DHC model [6–9], DHCV in zirconium alloys is governed by hydrogen diffusion and the hydrogen concentration gradient at a flaw tip defined by the supersaturated hydrogen concentration, the yield strength and the threshold stress intensity factor

$$V = (k_1 D_H)\Delta C\left[k_2 \frac{\sigma_{YS}}{K_{IH}}\right]^2, \quad (1)$$

where V is the DHC velocity, D_H is a diffusivity of hydrogen, ΔC is a supersaturated hydrogen concentration, σ_{YS} is the yield strength of the CANDU tube used, k_1 and k_2 are constants and K_{IH} is the threshold stress intensity factor for the onset of DHC in the CANDU Zr–2.5Nb tube. Thus, since the supersaturated hydrogen concentration must be the same irrespective of the orientation, the ratio of the axial and radial DHCV can be determined as shown below:

$$\frac{V_{ax}}{V_r} = \frac{D_{H,ax}}{D_{H,r}}\left(\frac{\sigma_{YS,ax}}{\sigma_{YS,r}}\right)^2\left(\frac{K_{IH,r}}{K_{IH,ax}}\right)^2, \quad (2)$$

where V_{ax} and V_r are the DHC velocity in the axial and radial directions of the CANDU Zr–2.5Nb tube, $\sigma_{YS,ax}$ and $\sigma_{YS,r}$ are its axial and radial yield strengths, and $K_{IH,ax}$ and $K_{IH,r}$ are the axial and radial threshold stress intensity factors. A rationale for using the yield strengths in the crack growth directions instead of that in the tangential direction is that the DHC velocity changes with the cracking direction (Fig. 4) even in the same cracking plane with the same stress being applied. Since it was demonstrated that the yield strengths of the CANDU Zr–2.5Nb tube are almost the same in both directions [5], Eq. (2) shows that the anisotropic DHCV depends only upon hydrogen diffusion and K_{IH} with the orientation. A problem arises in which of the D_H and K_{IH} shown in Eq. (2) controls DHCV. From the results shown in Fig. 5, the ratio of the axial and radial K_{IH} turned out to be 1.43. By placing this value into Eq. (2), we could suggest that the around two times higher V_{ax} than V_r is due to the higher radial K_{IH} than the axial K_{IH} as shown in Fig. 5 assuming the same hydrogen diffusivity with the orientation of the CANDU pressure tube. However, this hypothesis disagrees with Skinner's experiment [15] showing an anisotropic hydrogen diffusion between the circumferential and axial directions of a Pickering tube. Further, by evaluating the quantitative contribution of a hydrogen diffusivity and the hydrogen concentration gradient to DHCV of Zr–2.5Nb tubes with different distributions of the β-Zr phase, Kim demonstrated that higher DHCV of the CANDU tube with a semi-continuous β-Zr phase when compared to that of the RBMK Russian tube with a fully discontinuous β-Zr phase is dominantly caused by the hydrogen diffusivity at temperatures below 300 °C [9]. Hence, a more reasonable rationale is that the DHC crack growth rate is governed primarily by a hydrogen diffusivity as Kim has already demonstrated experimentally and the effect of K_{IH} on DHCV that governs the hydrogen concentration gradient at the flaw tip, is relatively minor at below 300 °C compared to diffusion of hydrogen.

Another decisive evidence for this rationale can be provided by demonstrating that the anisotropic DHCV of the CANDU Zr–2.5Nb tube should disappear by causing the β-Zr phase to become uniformly distributed with its orientation. It is because a hydrogen diffusivity or D_H is influenced mainly by the distribution of the β-Zr where hydrogen diffuses much faster when compared to the α-Zr [15,16]. Fortunately, Levi and Sagat [10] conducted this kind of experiment where the axial and radial DHCV's were measured from both a CANDU Zr–2.5Nb tube annealed at 400 °C for 1000 h and a Zr–2.5Nb plate annealed at 650 °C for 9 h. Fig. 6 shows their results where the T–R or T–ST specimens with the crack growing in the radial direction of the tube or the plate, respectively, had the similar growth rate to that of the T–L specimens with the crack growing in the axial direction. As expected, no anisotropic DHCV with the orientation was observed for the annealed Zr–2.5Nb tube and plate where a non-uniform distribution of the β-Zr should be disrupted by annealing to become uniform. In other words, a difference in DHCV with the orientation disappeared over a temperature range of 100–250 °C. It should be noted that the textures of the Zr–2.5Nb plate and tube remain unaffected by annealing even at 650 °C. Despite the anisotropic K_{IH} effect being persistent as shown in Fig. 5, the isotropic DHCV of the annealed Zr–2.5Nb tube and plate as shown in Fig. 6 reveals that the K_{IH} effect on the anisotropic DHCV is relatively trivial at below 300 °C. Thus, from the anisotropic DHCV shown in Fig. 4, we can conclude that the axial D_H in a CANDU Zr–2.5Nb tube is around 1.8–2 times higher than the radial D_H. This conclusion looks plausible accounting for Skinner's experiment that the ratio of the axial D_H and the transverse one in a Pickering tube ranged from 1.5 to 1.8 in the same temperature range of 160–250 °C where the DHC tests were carried out in this study. In essence, the results shown in Fig. 6 provide supportive evidence for the plausibility of Kim's DHC model that DHCV of the CANDU Zr–2.5Nb tubes at temperatures below 300 °C is governed primarily by a hydrogen diffusivity and secondarily by the hydrogen concentration gradient regulated by the yield strength, K_{IH}, and the supersaturated hydrogen concentration.

3.2. Variation of DHCV and its anisotropy along irradiated CANDU tubes

It is generally acknowledged that the CANDU Zr–2.5Nb pressure tubes undergo a microstructural evolution such as a decomposition of the β-Zr phase during their operation in reactors. To understand the decomposition behavior of the β-Zr with the operating temperature and fast neutron fluence, the Nb concentration in the β-Zr

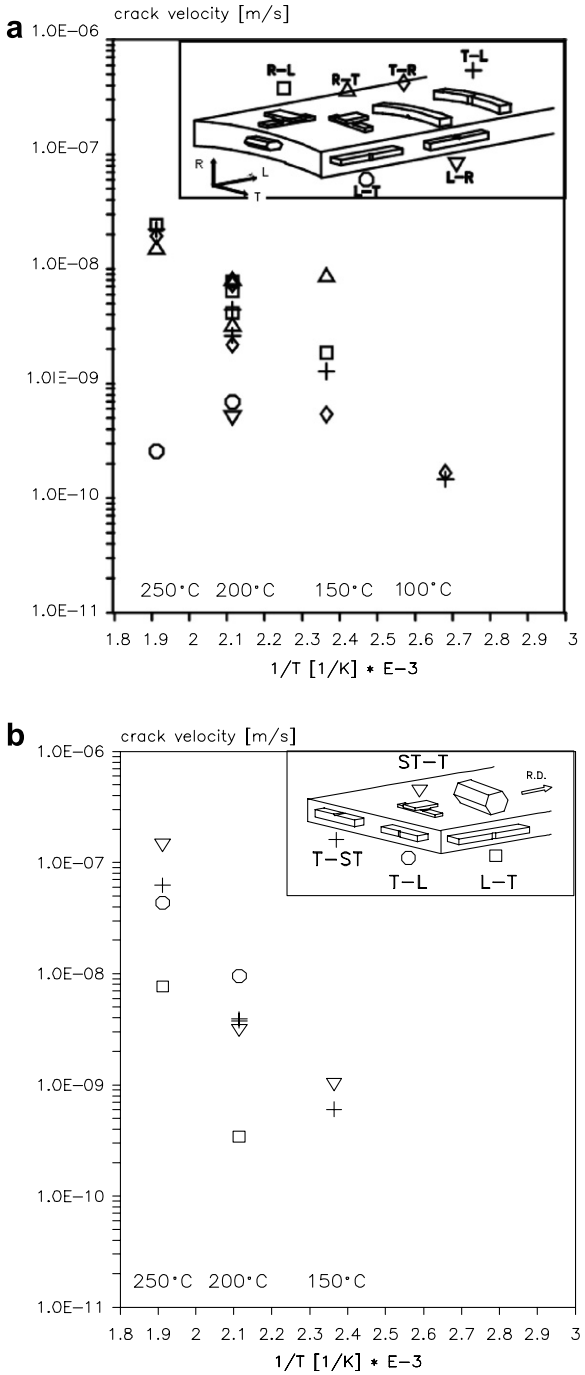

Fig. 6. DHCV with the orientation in (a) a Zr–2.5Nb tube annealed at 400 °C for 1000 h and (b) a Zr–2.5Nb plate annealed at 650 °C for 9 h (Courtesy of Levi and Sagat; see also Ref. [10], Figs. 3 and 8).

grains, as a measure of the β-Zr decomposition [17], were determined at the following three locations of the irradiated Zr–2.5Nb tube that was discharged after a 10 year operation in a reactor: the inlet, the middle and the outlet regions. As shown in Table 1 [18], the outlet and inlet regions were exposed to the highest and lowest temperatures, respectively, while the middle region had the highest neutron fluence ($E > 1$ MeV). To examine the Nb concentrations in the β-Zr grains with a higher confidence, a carbon replica method was applied to extract the β-Zr grains only, as shown in Fig. 7, whose compositions were determined by the energy dispersive X-ray analysis (EDX). As shown in Fig. 8, the Nb concentration in the β-Zr grains

Table 1
Operating conditions of the examined regions of the CANDU Zr–2.5Nb tube [18]

Location	Distance from the inlet (cm)	Coolant temperature (°C)	Fast neutron fluence ($E > 1$ MeV) ($\times 10^{25}$ n/m^2)
Inlet	173–190	275.4	7.66
Middle	266–283	285.5	8.91
Outlet	456–483	302.1	6.84

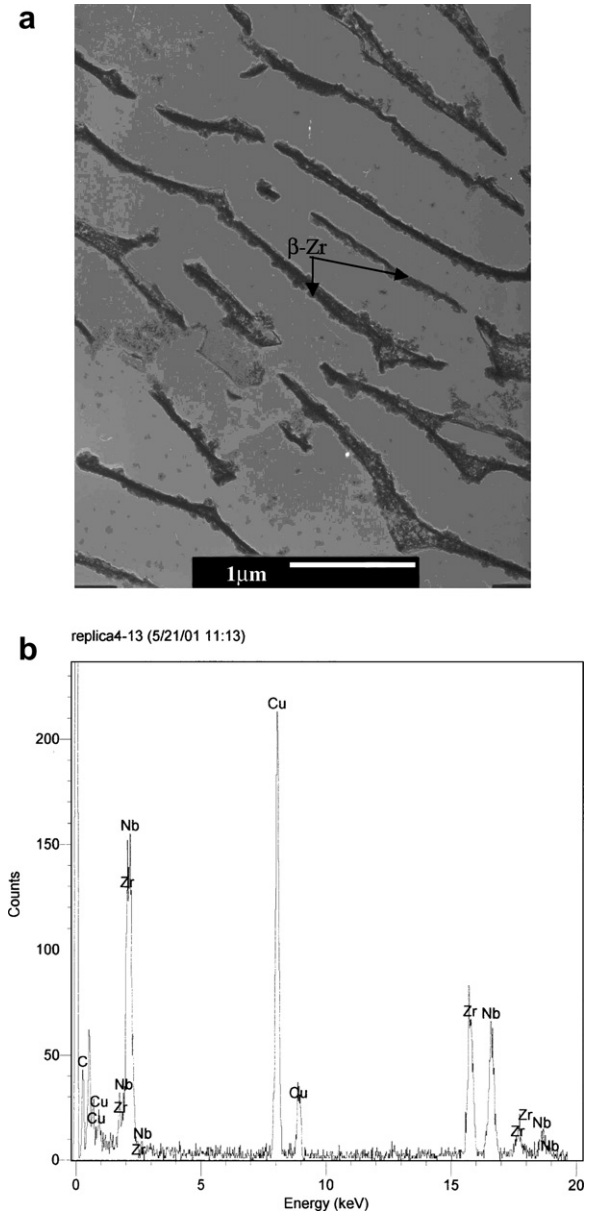

Fig. 7. Micrograph of the β-Zr phase extracted from Zr–2.5Nb pressure tube by a carbon replica film (a) and the EDX analysis of the extracted β-Zr phase (b).

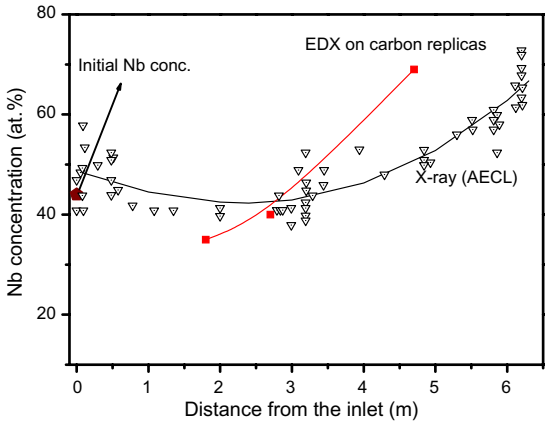

Fig. 8. Distribution of the Nb content in the β-Zr phase with a distance from the inlet of the irradiated Z–2.5Nb tubes determined by the carbon replica method (■) along with that by the X-ray diffraction analysis (▽) [20]: the Zr–2.5Nb tube used for the carbon replica method had been discharged after 10 years of service from Wolsong Unit 1 while those used for the X-ray analysis had been in reactor service for 2–14 years in Canadian reactors [20].

increased linearly with the distance from the inlet. In other words, the outlet region exposed to the highest temperature had the highest Nb concentration of 69 at.% Nb in the β-Zr due to a thermal decomposition, possibly leading to a fully discontinuous distribution of the β-Zr as observed on the unirradiated tubes by thermal annealing [9,16]. In contrast, the inlet region had little thermal decomposition of the β-Zr but it rather had the α-Zr grains supersaturated with the Nb atoms due to radiation enhanced dissolution [18,19]. Thus, it seems that the distribution of the β-Zr grains is maintained as semi-continuous at the inlet region, and becomes more discontinuous from the inlet towards the outlet region. This change of the distribution of the β-Zr grains from the inlet towards the outlet region will cause DHCV to decrease linearly along the irradiated tube with inlet regions of higher DHCV. In support of this hypothesis is Sagat's experiment [2] demonstrating that the inlet region has two times higher DHCV when compared to the outlet part and that DHCV decreases from the inlet region towards the outlet region. Furthermore, an outlet region with a fully discontinuous distribution of the β-Zr will lead to the same DHCV with the orientation, which is verified by Sagat's experiment where the radial and axial DHCV's have the same value at 300 °C but $V_r > V_{ax}$ at lower temperatures [2]. No anisotropic DHCV at the outlet region is another evidence that the Nb concentration in the β-Zr represents a measure of the disrupted distribution of the β-Zr grains by thermal decomposition, which was revealed experimentally for the unirradiated Zr–2.5Nb alloys by Levi and Sagat (Fig. 6).

It should be noted that the Nb concentration distribution along the tube determined by the carbon replica method differs from that determined by the X-ray diffraction analysis, as shown in Fig. 8. This difference may result either from different analytical methods or from different operating conditions of the examined pressure tubes used by Griffiths and us. It is surprising to see that despite different operating conditions of the pressure tubes, our data showing a linear increase of the %Nb in the β-Zr along the tube length from the inlet predicts a linear decrease of DHCV along the tube length as Sagat demonstrated for their irradiated tubes [2]. In contrast, the distribution of the %Nb along the tube reported by Griffiths cannot provide a plausible explanation for that of their DHCV along the length. Through a more controlled experiment where DHCV and the %Nb in the β-Zr were measured at the same regions of an irradiated CANDU tube such as the inlet, middle and outlet regions, Griffiths recently argued that the maximum DHCV occurring somewhere in the lower half position of the tube is due to the decomposition behavior of the β-Zr as a function of the axial location [17]. However, his argument cannot account for the reason why the position with the maximum DHCV disagrees with the position with the lowest %Nb in the β-Zr, corresponding to the center of the tube.

4. Conclusions

DHCV of an unirradiated CANDU Zr–2.5Nb tube was two times higher in the axial direction than that in the radial direction over a temperature range of 160 to 250 °C. Threshold stress intensity factor, K_{IH} for the onset of delayed hydride cracking was lower in the axial direction than that in the radial direction and the ratio of the radial and axial K_{IH} was constant at temperatures ranging from 160 to 280 °C. According to Kim's DHC model where DHCV is governed primarily by a hydrogen diffusivity and secondarily by the hydrogen concentration gradient determined at below 300 °C, therefore, we conclude that the higher axial DHCV of the CANDU Zr–2.5Nb tube is caused by higher hydrogen diffusivity in the axial direction, and not affected by K_{IH} with the tube orientation. Experimental evidence to this conclusion is given by citing Levi and Sagat's experiment where Zr–2.5Nb tubes or plates with a fully discontinuous β-Zr due to annealing at 400 °C for 1000 h or 650 °C for 9 h showed no anisotropic DHCV with the orientation. Thermal decomposition of the β-Zr occurred in the irradiated CANDU Zr–2.5Nb tube, which was highest at the outlet region with 69 at.% Nb due to thermal annealing and arose little at the inlet region due to radiation enhanced dissolution. The disrupted distribution of the β-Zr accompanying a thermal decomposition accounts for the linear decrease of DHCV of irradiated CANDU tubes from the inlet region towards the outlet region and the disappearance of an anisotropic DHCV at 300 °C. Consequently, we conclude that Kim's DHC model is plausible.

Acknowledgements

This work has been carried out as part of the Nuclear R&D program supported by Ministry of Science and Technology, Korea. One of the authors would like to express his

sincere thanks to Dr M.R. Levi for his permission to present his results in this paper.

References

[1] A.R. Causey, V.F. Urbanic, C.E. Coleman, J. Nucl. Mater. 71 (1977) 25.
[2] S. Sagat, C.E. Coleman, M. Griffiths, B.J.S. Wilkins, in: Proceedings of the 10th Symposium on Zirconium in the Nuclear Industry, ASTM STP 1245, 1994, p. 35.
[3] R. Dutton, K. Nuttal, M.P. Puls, L.A. Simpson, Met. Trans. 8A (1977) 1553.
[4] M.P. Puls, L.A. Simpson, R. Dutton, in: L.A. Simpson (Ed.), Fracture Problems and Solutions in the Energy Industry, Pergamon, Oxford, 1982, p. 13.
[5] Y.S. Kim, S.S. Kim, S.C. Kwon, K.S. Im, Y.M. Cheong, Met. Trans. 33A (2002) 919.
[6] Y.S. Kim, et al., in: Abstract Booklet for 14th Symposium on Zirconium in the Nuclear Industry, ASTM, Stockholm, Sweden, 2004, p. 81.
[7] Y.S. Kim, Met. Mater. Int. 11 (2005) 29.
[8] Y.S. Kim, K.S. Kim, Y.M. Cheong, J. Nucl. Sci. Tech. 43 (2006) 1120.
[9] Y.S. Kim, Mater. Sci. Eng. A (2007), doi:10.1016/j.msea.2006.09.123.
[10] M.R. Levi, S. Sagat, in: Proceedings of the International Symposium on Environmental Degradation of Materials and Corrosion Control in Metals, 38th Annual Conference of Metallurgists, 29th Annual Hydrometallurgical Meeting of CIM, Quebec, 1999.
[11] Y.S. Kim, et al., KAERI/TR-1329/99, Korea Atomic Energy Research Institute, Daejeon, 1999.
[12] Y.S. Kim, S.J. Kim, K.S. Im, J. Nucl. Mater. 335 (2004) 387.
[13] S.J. Kim, Effect of Heat Treatment on Delayed Hydride Cracking Behavior of Zr–2.5%Nb Alloy, Master Thesis, Korea University, 1999.
[14] S.S. Kim, Y.S. Kim, J. Nucl. Mater. 279 (2000) 286.
[15] B.C. Skinner, R. Dutton, in: N.R. Moody, A.W. Thompson (Eds.), Hydrogen Effects on Material Behavior, The Minerals, Metals and Materials, 1990, p. 73.
[16] L.A. Simpson, C.D. Cann, J. Nucl. Mater. 126 (1984) 70.
[17] M. Griffiths, P.H. Davies, W.G. Davies, S. Sagat, in: Proceedings of the 13th Symposium on Zirconium in the Nuclear Industry, in: G.D. Moan, P. Rudling (Eds.), ASTM STP, 1423, ASTM, 2003, p. 507.
[18] Y.S. Kim, K.S. Im, Y.M. Cheong, S.B. Ahn, J. Nucl. Mater. 346 (2005) 120.
[19] R.S. Nelson, J.A. Hudson, D.J. Mazey, J. Nucl. Mater. 44 (1972) 318.
[20] M. Griffiths, J.F. Mecke, J.E. Winegar, in: Proceedings of the 11th Symposium on Zirconium in the Nuclear Industry, ASTM STP 1295, 1996, p. 580.